IL NUOVO CIMENTO Vol. 37 C, N. 4 Luglio-Agosto 2014
DOI 10.1393/ncc/i2014-11802-7

Communications: SIF Congress 2013

Proof of concept of an innovative detector for nuclear imaging applications

G. Pirrone on behalf of the INFN 4DMPET Collaboration

Dipartimento di Fisica, Università di Pisa and INFN, Sezione di Pisa
Largo B. Pontecorvo 3, 56127 Pisa, Italy

ricevuto il 3 Febbraio 2014; approvato il 19 Marzo 2014

Summary. — The 4DM-PET experiment aims to develop an innovative detector module for PET applications. The detector is based on a $20 \times 20 \times 10\,\mathrm{mm}^3$ LYSO monolithic scintillator crystal coupled on the large opposite surfaces to 4×4 Silicon Photomultiplier pixel matrices of 5 mm pitch. The Detector is connected to a custom designed Front-End ASICs managed by an FPGA-based read-out system. This configuration allows measuring the Depth of Interaction of gamma photons interacting in the crystal volume. To test the spatial resolution capabilities of this module the detector has been scanned with a pencil beam produced by collimated radioactive sources along the three dimensions of the crystal block. The results of the prototype characterization in terms of spatial resolution in the x-y plane and the Depth Of Interaction resolution are presented here.

PACS 29.40.-n – Detector radiation.
PACS 87.57.-s – Medical imaging.
PACS 87.57.cf – Spatial resolution.
PACS 87.57.uk – Positron Emission Tomography (PET).

1. – Introduction

Positron Emission Tomography (PET) is a nuclear medical imaging technique whereby a compound labeled with a positron emitting nuclide is injected into the body to provide tomographic images of the radioisotope concentration in the patient tissues. The main goal of PET is to provide functional information as accurate as possible, maintaining a low dose to the patient. For this reason, one of the most important features in PET is the spatial resolution.

Spatial resolution in PET scanners is limited by the positron range in the tissue and non-collinearity of the annihilation photons on one side and by the technology of the detectors.

Since the positron physics is the ultimate limit of the PET technique, it is of utmost importance finding new methods to improve the detector performance. In commercial

PET scanners the detectors are based on pixellated crystals coupled to arrays of photodetectors and the impact position of the annihilation gammas on the detector surface is obtained appying a coding algorithm. For this kind of detectors the spatial resolution is limited by the crystal pitch, the coding error and the parallax error [1, 2].

The crystal pitch is the dominant contribution to the detector spatial resolution. This effect is due to the limited solid angle coverage of the crystals involved in the photons detection. Hence the line connecting the two crystals in a detector pair (Line Of Response or LOR) can be determined with an error of $d/2$, where d is the width of the detector element.

The coding error is due to an incorrect identification of the crystal where the annihilation photons interact. In fact, in order to reduce the number of electronics channels, the detector has more scintillation crystals than photodetector elements.

Parallax error occurs when photons interact at a finite depth within the crystal. Since in the present detectors the Depth Of Interaction (DOI) is not measured, reconstructed LORs are affected by un uncertainty that increases moving from the centre of the Field Of View (FOV).

The detector concept presented here is based on a monolithic scintillating crystal read by two arrays of SiPMs placed on the two opposite faces of the crystal [3]. With respect to the pixxellated crystal approach the use of monolithic block allow to overcome the problem of the coding error and the limitation of the pixel size. The photon hit position in the plane x-y is obtained using the centre-of-gravity method [4, 5], and the spatial resolution is limited by the granularity of the photodetectors and by the amount of light collected, mainly at the borders of the crystal. Moreover, the light emitted by the scintillator crystal is collected by the two tiles of SiPMs and this allow measuring the Depth Of Interaction.

Furthermore the use of the Silicon Photomultiplier (SiPM) makes the proposed module extremely compact and magnetic field compatible for a possible integration in a PET/MR hybrid scanner [6-8].

The 4DMPET experiment of the INFN aims to implement the detector concept described above. The final design foresee a $48 \times 48 \times 10\,\mathrm{cm}^3$ LYSO block read-out on both sides by 16×16 SiPMs, $3 \times 3\,\mathrm{mm}^2$ each. Custom designed front-end ASICs will provide for each side the energy and time related to the event and a local FPGA will perform the data preprocessing in order to reduce the transmission bandwith to the acquisition system.

2. – Materials and methods

A detector prototype was made upon the same conceptual design of the module described above. The detector is based on a $20 \times 20 \times 10\,\mathrm{mm}^3$ LYSO continuous crystal read by two SiPMs matrices (called tiles hereafter) on the opposite larger surfaces (fig. 1). Each matrix is composed of 4×4 Silicon Photomultiplier pixel ($4 \times 4\,\mathrm{mm}^2$ each) of 5 mm pitch. A water-based cooling system has been used to stabilize the temperature at 18 °C.

To avoid internal reflections and improve the spatial resolution performance of the prototype, LYSO crystal is painted black on the lateral surfaces not facing the SiPM matrices.

Every SiPM is connected to a custom designed front-end ASICs (BASIC 32) [9] read-out by a Xilinx ML605 evaluation board which hosts a Virtex 6 FPGA clocked at 200 MHz. The acquisition board communicates with a PC through the GIGAbit Ethernet Protocol. The acquisition and online monitoring software is written in LabVIEW [10].

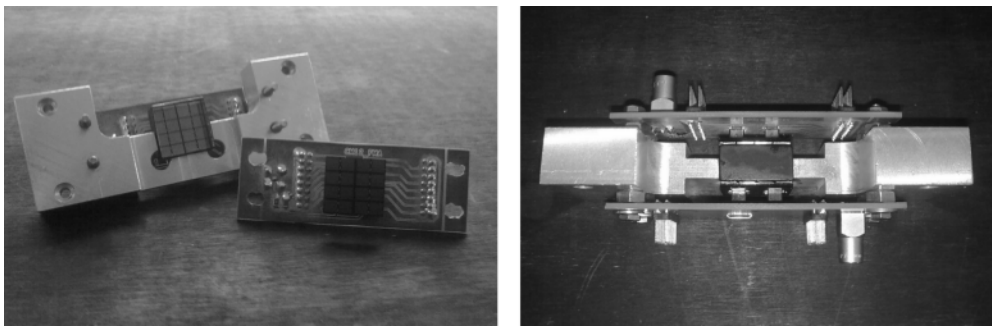

Fig. 1. – In the left picture the tiles plugged on detector boards and the larger surface of the crystal block are shown. In the right picture the assembled prototype is shown.

To assess the spatial resolution capabilities of the module, the block has been scanned with a pencil beam along the three dimensions. The collimated pencil beam has been obtained by using a ^{22}Na source and selecting the coincidence events between the block and a small detector composed on a $1 \times 1 \times 10\,\mathrm{mm}^3$ white painted LYSO crystal coupled to $1 \times 1\,\mathrm{mm}^2$ SiPM. The ^{22}Na radioactive source and the single detector are fixed to a rigid support at 35 mm distance one to the other. A couple of linear stages is used to move the source-single detector assembly. Figure 2 shows the scheme of the experimental set-up.

For each acquisition, when an interaction event occurs in the crystal, a cluster of SiPMs on the top and bottom tiles activates. An iterative algorithm of *Cluster Finding* that operates in two steps has been developed. The first one is the search on both tile of the highest recorded signal in a scintillation event (the seed). The pixel is selected if its value is greater than a threshold $T_H = n \times \sigma_{ped_i}$, where σ_{ped_i} is the standard deviation of the pedestal of the i-th channel. The second step is the looks for neighboring pixels to add to the seed; this occurs when their values are greater than another threshold $T_L = m \times \sigma_{ped_j}$, where σ_{ped_j} has the same meaning described above. Pixels are added to the cluster until the cluster dimension remains constant. After an optimization process of the detector efficiency n was set at 5 while m was set at 3.

To test the detector spatial resolution a total scan of the x-y plane with a pitch of 2 mm has been performed. For each selected cluster, the centre of gravity (COG) method

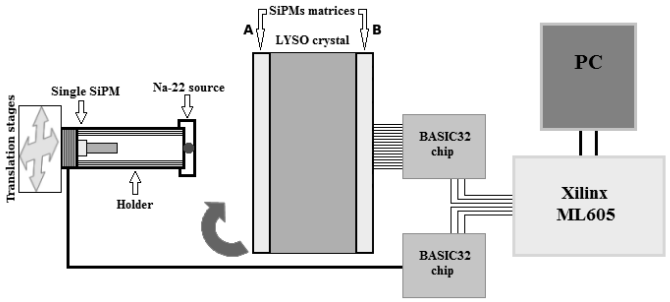

Fig. 2. – Scheme of the experimental set-up.

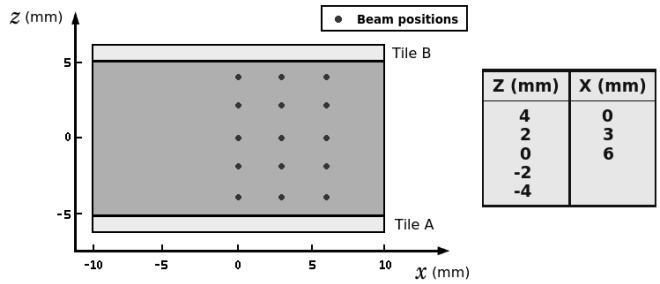

Z (mm)	X (mm)
4	0
2	3
0	6
-2	
-4	

Fig. 3. – Real positions of the pencil beam on the lateral surface of the crystal. Symmetry for $x < 0$ has been supposed.

has been applied to reconstruct the photon hit position, and the spatial resolution has been obtained measuring the width of the distributions profile for the x and y directions.

To measure the Depth Of Interaction the detector has been rotated to scan the lateral surface of the crystal. The beam has been aimed to five different positions along the z-direction and in three different positions along the x direction. The beam positions are shown in fig. 3.

The Depth Of Interaction of the photons can be determined in an event considering the asymmetry of the cluster size on the two opposite tiles, being the cluser size the number of active SiPMs in a cluster. Due to geometrical distribution of the scintillation light and to critical angle, clusters closer to the photon interaction point have a smaller number of pixels than the corresponding in the opposite face. Therefore this parameter is related to the DOI information and it can be estimated using the approximate formula [10, 11]:

$$DOI \propto \frac{D}{2}\frac{C\mathrm{Size}_A - C\mathrm{Size}_B}{C\mathrm{Size}_A + C\mathrm{Size}_B} \tag{1a}$$

where $C\mathrm{Size}_A$ and $C\mathrm{Size}_B$ are the cluster sizes of both matrices while D is the is the crystal thickness.

No correction has been done to take into account the dimension of the beam spot in the data analysis.

This work was conducted in three steps that can be summarized in the experimental set-up design, the data acquisition and the data analysis, where my personal contribution concerned the last two tasks. In particular I acquired the data in the different geometries described above and developed the recursive algorithm used in the data analysis for the selection of the events.

3. – Experimental results

3˙1. *Detector spatial resolution.* – The x-y distributions at the centre of the module are shown in fig. 4. A spatial resolution (FWHM) of 1.9 mm for the tile A and 1.8 mm for the tile B has been obtained.

Figures 5 (tile A) and 6 (tile B) show the difference between the reconstructed positions *versus* the real positions (beam positions). For the tile A the points in a residual plot are not randomly dispersed around the horizontal axis (dashed line) and the mean of the residuals (pointed line) is not equal to zero. For the tile B the residual plot shows

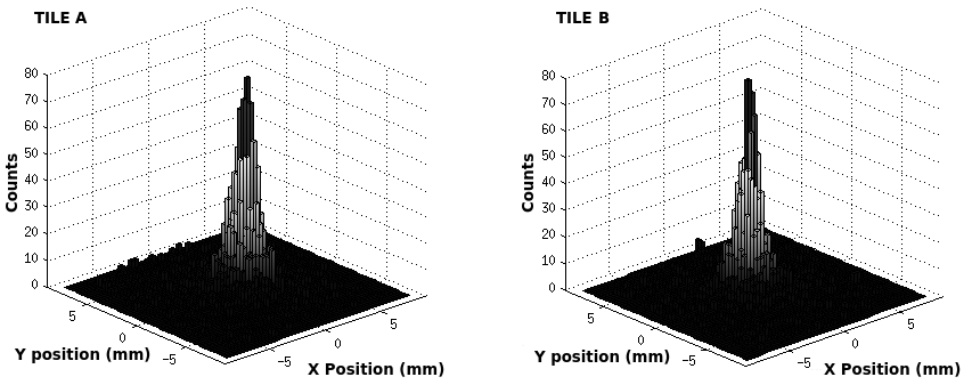

Fig. 4. – 3D reconstruction of x-y distribution of the events with the beam at the centre of the module for tile A (on the left) and tile B (on the right).

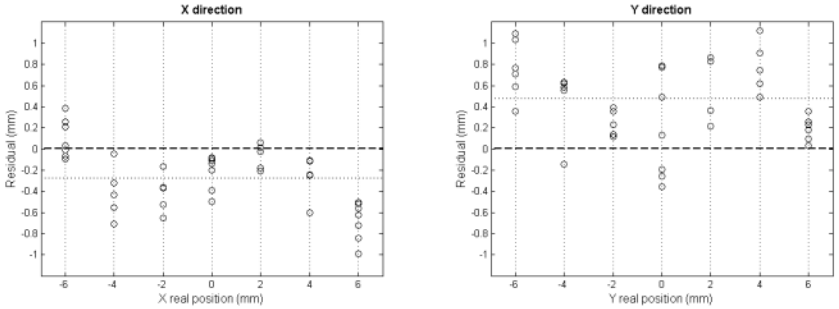

Fig. 5. – Tile A - Residual plot for the x and y directions as a function of the real positions.

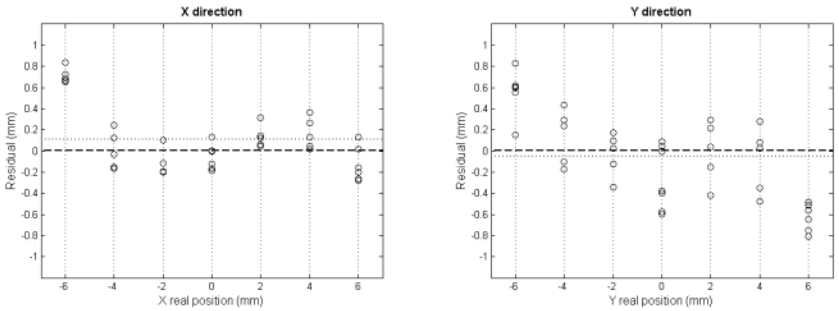

Fig. 6. – Tile B - Residual plot for the x and y directions as a function of the real positions.

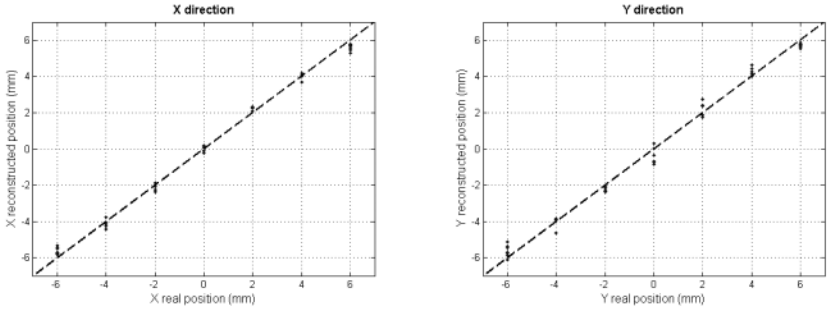

Fig. 7. – Tile A - Reconstructed positions in the x and y directions as a function of the real position of the beam.

a fairly random pattern and the mean of the residuals is approximately zero. The different results obtained are due to the misalignment of the two tiles and that introduces a systematic error, hence a correction to the data has been done.

Figures 7 and 8 show the reconstructed positions as a function of the real position of the beam. The dashed lines show the 45° line represents the ideal case of the exact position reconstruction. In the four central pixels of both tiles a linear model provides a good fit to the data.

The reconstructed positions for both tiles are shown in fig. 9. In the central region of the detector the photons interaction points are well determined using the COG method, while the information in the regions close to the detector edges is lost due to the lower scintillation light collected by the SiPMs.

3˙2. *Depth Of Interaction.* – The mean and the standard deviation of the distribution of DOI (eq. (1)) have been plotted as a function of the real beam position along the z axis. They are shown in fig. 10, where the error bars in the real position are due to the beam spot size and the dotted line is the bisectors that shows an exact correspondence between the real positions and the Depth Of Interaction estimation.

For the acquisitions in $X = 0\,\text{mm}$ and $X = 3\,\text{mm}$ there is a linear relationship between the reconstructed and real positions and the standard deviation of the asymmetry

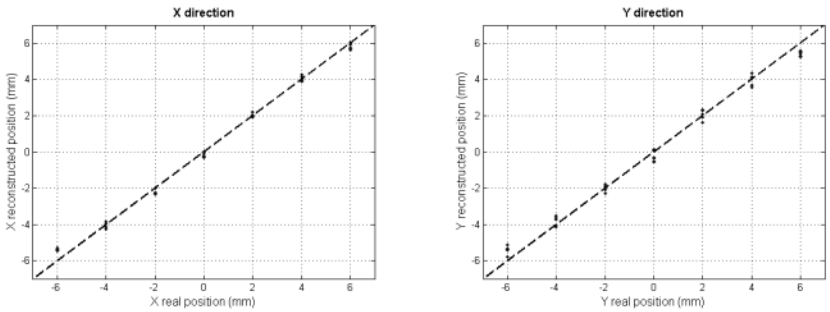

Fig. 8. – Tile B - Reconstructed positions in the x and y directions as a function of the real position of the beam.

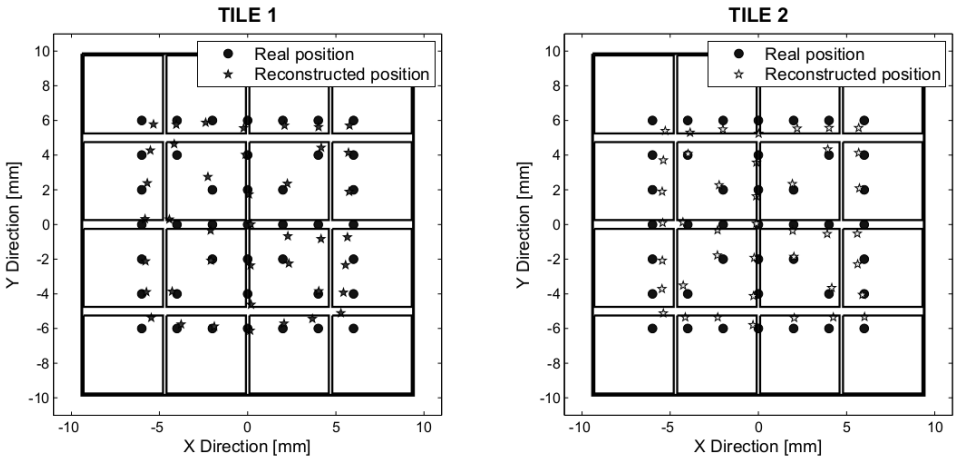

Fig. 9. – Real (blu) and reconstructed positions (red) in a scan of 2 mm for tile A (on the left) and tile B (on the right). The black lines defines the SiPMs of each matrix.

distributions goes from 1.8 mm for central positions to 2.4 mm for positions close to the tiles. Instead for the acquisitions in $X = 6$ mm the beam is near the corner of the detector and the information about the interaction point worsens because the edge effects are predominant.

The high value of the standard deviation depends first of all on the large dimension of the SiPMs (that implies a low number of pixels involved in the cluster). Another contribution is given by the dead area among adjacent SiPMs and finally by the beam spot size.

The Depth Of Interaction results shown above for this detector are fully comparable with the results obtained in the simulation [11].

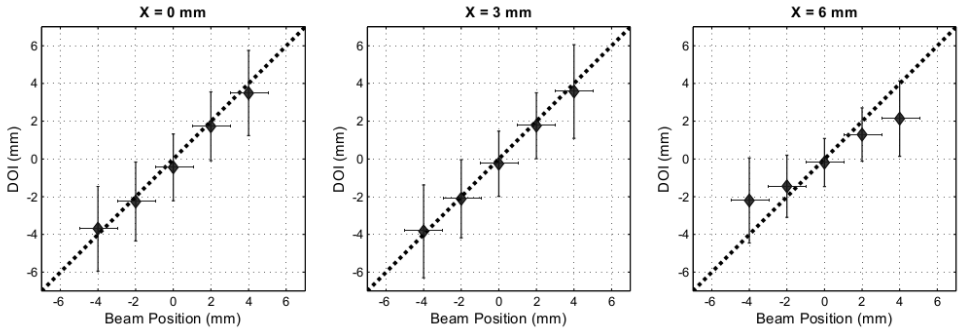

Fig. 10. – Depth Of Interaction estimation as a function of the z beam position in $X = 0$ mm, $X = 3$ mm and $X = 6$ mm.

4. – Conclusions

A first 4DMPET prototype based on a $20 \times 20 \times 10\,\mathrm{mm}^3$ monolithic scintillator crystal coupled to 4×4 SiPMs matrices has been realized and the performances have been tested in terms of spatial and Depth Of Interaction resolution.

A spatial resolution (FWHM) of about 2 mm in the x-y plane has been obtained. The photon hit positions in this plane are well reconstructed in the four central SiPMs of both tiles, safe for the regions close to the detector edges where a correction method is required.

The DOI in the central part of the detector is proportional to the cluster asymmetry and the standard deviation is about 2 mm. Nevertheless, a different DOI reconstruction method must be implemented to take into account the edge effects.

Better performance can be expected in the final 4D-MPET module. The detector is under developing and it is based on a $50 \times 50 \times 10\,\mathrm{mm}^3$ monolithic crystal read by two SiPM matrices. Each matrix is composed of 16×16 square Silicon Photomultiplier of 3 mm side. With this configuration, it has been obtained in simulation an overall error in the 3D reconstructed interaction point of about 1 mm [12].

* * *

This work has been supported by the 4DMPET INFN (sections of Bari, Perugia, Torino and Pisa) collaboration and the INSIDE project.

REFERENCES

[1] Derenzo S. E. and Moses W. W., *Critical instrumentation issues for resolution < 2 mm, high sensitivity brain PET*, in *Quantification of Brain Function, Tracer Kinetics and Image Analysis in Brain PET*, edited by Uenura *et al.* (Elsevier) 1993, pp. 25-40.
[2] Moses W. W., *Nucl. Instrum. Methods Phys. Res. A*, **648** (2011) S236.
[3] Marino N. *et al.*, *J. Instrum.*, **7** (2012) C08003.
[4] Moehrs S. *et al.*, *Phys. Med. Biol.*, **51** (2006) 1113.
[5] Llosa G. *et al.*, *Phys. Med. Biol.*, **55** (2010) 7299.
[6] Schaart D. R. *et al.*, *Phys. Med. Biol.*, **54** (2009) 3501.
[7] Kolb A. *et al.*, *Phys. Med. Biol.*, **55** (2010) 1815.
[8] Zaidi H. and Del Guerra A., *Med. Phys.*, **38** (2011) 5667.
[9] Marzocca C., *BASIC32: development of a multichannel readout ASIC for SiPM detectors*, in *The Eighth International Meeting on Front-End Electronics* (Bergamo, Italy) 2011.
[10] Morrocchi M. *et al.*, *Nucl. Instrum. Methods Phys. Res. A*, **732** (2013) 603.
[11] Pennazio F. *et al.*, *SiPM-based PET module with Depth Of Interaction*, in *Nuclear Science Symposium and Medical Imaging Conference (NSS/MIC)* (IEEE) 2012.
[12] Cerello P. *et al.*, *Nucl. Instrum. Methods Phys. Res. A*, **702** (2013) 6.